Elucidating the structure of chiral molecules by using amplified vibrational circular dichroism: from theory to experimental realization

Domingos, S.R.; Hartl, F.; Buma, W.J.; Woutersen, S.

DOI
10.1002/cphc.201500551

Publication date
2015

Document Version
Final published version

Published in
ChemPhysChem

ChemPubSoc Europe

DOI: 10.1002/cphc.201500551

CHEMPHYSCHEM Concepts

Elucidating the Structure of Chiral Molecules by using Amplified Vibrational Circular Dichroism: From Theory to Experimental Realization

Sérgio R. Domingos,[a, c] František Hartl,*[b] Wybren Jan Buma,*[a] and Sander Woutersen*[a]

Recent experimental observations of enhanced vibrational circular dichroism (VCD) in molecular systems with low-lying electronically excited states suggest interesting new applications of VCD spectroscopy. The theory describing VCD enhancement through vibronic coupling schemes was derived by Nafie in 1983, but only recently experimental evidence of VCD amplification has demonstrated the extent to which this effect can be exploited as a structure elucidation tool to probe local structure. In this Concept paper, we give an overview of the physics behind vibrational circular dichroism, in particular the equations governing the VCD amplification effect, and review the latest experimental developments with a prospective view on the application of amplified VCD to locally probe biomolecular structure.

1. Introduction

Chirality plays a key role in chemistry and biology. The discovery of molecular chirality emerged from a series of observations of optical activity by Argo and Biot (1811), Herschel (1822), Pasteur (1848), van 't Hoff and Le Bel (1874) and Lord Kelvin (1904). Since then, the connection between molecular handedness related to mirror-image molecules and optical activity has been well established. Two non-superimposable mirror-image isomers of a chiral molecule, similar to our right and left hands, are referred to as enantiomers. Most biomolecules are chiral and thus have a stereoselective bias for specific biochemical interactions. Because of this bias, different enantiomers may exhibit completely different biological activities. It is precisely for this reason that the unambiguous assignment of enantiomers is a key aspect of stereochemistry, with increased importance in pharmaceutical research, even more so because of the stringent rules imposed nowadays by regulatory agencies on specifications of enantiomeric identity and purity.

Vibrational circular dichroism (VCD), that is, the differential absorption, $\Delta A = A_L - A_R$, for left and right circularly polarized infrared light is a powerful technique for this purpose because it makes it possible to determine the absolute configuration and conformation (or distribution of conformations) of a chiral molecule without reference to empirical rules. Due to the pioneering work of Stephens, Nafie, Keiderling, and many others during the past two decades, VCD has emerged as a tool for structure elucidation of chiral molecules in the condensed phase and is nowadays an established technique used routinely in many chemical and biochemical laboratories.[1–3] The application of VCD as a probe of chiral molecular structure has in recent years received a boost due to significant experimental and theoretical progress. Instrumental advances have led to the development of commercial VCD spectrometers while the formulation and implementation of the theoretical expressions for calculating VCD intensities in quantum-chemical packages such as Gaussian[4] and ADF[5] allow for a direct comparison of experimentally recorded and theoretically predicted spectra. Such comparisons have by now become a robust method to determine the absolute structure and conformational heterogeneity of even complex mixtures of chiral molecules.

The applicability of VCD is nevertheless still limited in many cases by its signal intensities, which are typically four to six orders of magnitude smaller than that of the infrared absorption itself. One is thus required to work with highly concentrated samples, which may not be possible because of low solubility and aggregation of the sample. This limitation has seriously impeded extensive application of VCD, in particular for systems with biological relevance such as amino acids, peptides and proteins. In this paper, we show that one can overcome this drawback, not by improving the detection electronics, but by optimizing the "electronics" of the molecules, resulting in the amplification of VCD signals.

In the following we will first briefly review the physics that is at the basis of VCD, present the theoretical expressions for the intensities in a VCD spectrum, and rationalize why these intensities are generally very small. We will then consider under which conditions one may expect enhanced VCD intensities.

[a] Dr. S. R. Domingos, Prof. Dr. W. J. Buma, Prof. Dr. S. Woutersen
Van't Hoff Institute for Molecular Sciences, University of Amsterdam
Science Park 904, 1098 XH Amsterdam (The Netherlands)
E-mail: w.j.buma@uva.nl
s.woutersen@uva.nl

[b] Prof. Dr. F. Hartl
Department of Chemistry, University of Reading
Whiteknights, Reading RG6 6AD (United Kingdom)
E-mail: f.hartl@reading.ac.uk

[c] Dr. S. R. Domingos
Current address: Max Planck Institute for the Structure and Dynamics of Matter at the Center for Free-Electron Laser Science and The Hamburg Centre for Ultrafast Imaging, Universität Hamburg
Luruper Chaussee 149, 22671 Hamburg (Germany)

We will show that low-lying electronically excited states play a crucial role in this context, and review experimental observations from the past that already indicated that low-lying electronically excited states can lead to enhancement of VCD intensities. We will then proceed to more recent studies in which the electronic manifold of molecules is explicitly manipulated so as to optimize amplification of VCD intensities. From these studies it has become clear that the VCD enhancement is a localized phenomenon that offers a unique potential to serve as a local probe of chiral structure.

2. Theory of Vibrational Circular Dichroism

2.1. Classical Picture of CD

In a simple classical explanation of circular dichroism (CD),[6] the chiral molecule is modelled as a conducting coil (see Figure 1). In the scheme, the light wave propagates out of the paper and thus perpendicular to the coils. The electric field $\vec{E}$(t) and the magnetic field $\vec{B}$(t) both generate a current in the wire, the latter because of the magnetic flux through the coil changing with time (Lenz's Law). For right circularly polarized (RCP) light, the two currents have the same direction, whereas for left circularly polarized (LCP) light, they have opposite directions. Hence, a larger current is generated, and more energy dissipated ("light absorbed") in the coil for RCP light than for LCP light. Although this is a simplified explanation, it may be noted that a box filled with 1 cm long copper coils exhibits strong optical activity in the microwave region.[7]

2.2. VCD Intensity

VCD is the extension of CD to the infrared region of the electromagnetic spectrum, and is associated with the vibrational transitions of chiral molecules. The infrared absorbance can be related to the extinction coefficient $\varepsilon(\nu)$ by the Beer–Lambert law as $Abs = -log_{10}(\frac{I}{I_0}) = \varepsilon(\nu) \cdot l \cdot C$, where l and C are the length and concentration of the sample; I and I_0 designate transmitted and incoming light, respectively. The experimental parameter $\varepsilon(\nu)$ is related to the Einstein's coefficient for stimulated absorption between states i and f, B_{if}, by the following expression [Eq. (1)]:

$$A = \int \varepsilon(\nu) d\nu = \frac{h\nu_{fi}}{c} N_A B_{if} \tag{1}$$

where N_A is the Avogadro number, c the velocity of light in vacuum, and $\nu_{fi} = \Delta E_{fi}/h$. The quantity A on the left side of Equation (1) is the integrated molar absorption coefficient, that is, the area under the experimental infrared band. The VCD of a transition is defined as the differential absorption of left and right circularly polarized (LCP and RCP, respectively) infrared light passing through the sample, that is, the difference between the integrated molar absorption coefficients for LCP and RCP light. We can thus write the differential absorption coefficient ΔA as [Eq. (2)]:

$$\Delta A = A^{LCP} - A^{RCP} = \frac{h\nu_{fi}}{c} N_A (B_{if}^{LCP} - B_{if}^{RCP}) \tag{2}$$

The designations LCP and RCP indicate the handedness of the electric and magnetic field vector components as $+$ and $-$, respectively. Introducing the expressions for Einstein's stimulated emission coefficients[8] into Equation (2) leads to Equation (3):

$$\Delta A = (\frac{32\pi^3}{3})(\frac{\nu_{fi} N_A}{hc}) \mathrm{Im}\left[\langle \Psi_i | \vec{\mu}_{el} | \Psi_f \rangle \cdot \langle \Psi_f | \vec{\mu}_{mag} | \Psi_i \rangle\right] \tag{3}$$

where $\vec{\mu}_{el}$ and $\vec{\mu}_{mag}$ are the electric and magnetic transition-dipole moment operators, respectively, and $|\Psi_i\rangle$ and $|\Psi_f\rangle$ are the total wave functions for the initial and final states. The dot product of the two transition moments in Equation (3) is called the rotational strength, R_{if}, being thus defined as the imaginary part of the dot product between the electric and magnetic transition-dipole moments [Eq. (4)]:

$$R_{if} = \mathrm{Im}\left[\langle \Psi_i | \vec{\mu}_{el} | \Psi_f \rangle \cdot \langle \Psi_f | \vec{\mu}_{mag} | \Psi_i \rangle\right] \tag{4}$$

The differential absorption of LCP and RCP infrared light is therefore proportional to the rotational strength. For total wave functions $|\Psi_i\rangle$ and $|\Psi_f\rangle$ that are both real, R_{if} is a real quantity since $\vec{\mu}_{mag}$ is a purely imaginary operator. Hence, to evaluate the optical activity of a molecular system, one must include the magnetic interaction to describe nonzero VCD intensities, since R_{if} has its origin in the interference between electric and magnetic dipole transitions. Moreover, based on symmetry considerations, it can be shown that two enantiomers have rotational strengths of equal magnitude but opposite signs, the latter being determined by the angle between the electric and magnetic transition-dipole moments.

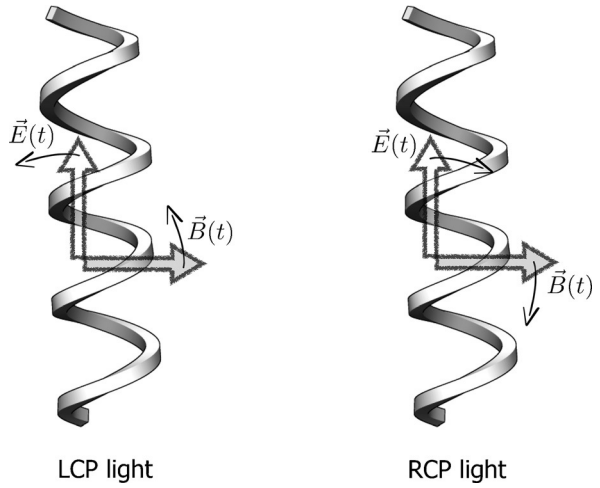

Figure 1. Classical picture of circular dichroism. The conducting helices represent the chiral molecules.

2.3. Prediction of the Rotational Strengths

Theoretical prediction of rotational strengths for infrared transitions in chiral molecules requires the calculation of the electric and magnetic transition-dipole moments associated with the operators $\vec{\mu}_{el}$ and $\vec{\mu}_{mag}$. For a transition between two vibrational states ($g \rightarrow e$) of a non-degenerate electronic state G, the electric and magnetic transition-dipole moments of a molecular system are given in the Born–Oppenheimer approximation by [Eqs. (5) and (6)]:

$$\begin{aligned}\langle \Psi_{Gg}|\vec{\mu}_{el}|\Psi_{Ge}\rangle &= \langle \chi_{Gg}|\langle \psi_G|\vec{\mu}_{el}|\psi_G\rangle|\chi_{Ge}\rangle \\ &= \langle \chi_{Gg}|\langle \psi_G|\vec{\mu}^{e}_{el}|\psi_G\rangle + \vec{\mu}^{n}_{el}|\chi_{Ge}\rangle\end{aligned} \quad (5)$$

$$\begin{aligned}\langle \Psi_{Gg}|\vec{\mu}_{mag}|\Psi_{Ge}\rangle &= \langle \chi_{Gg}|\langle \psi_G|\vec{\mu}_{mag}|\psi_G\rangle|\chi_{Ge}\rangle \\ &= \langle \chi_{Gg}|\langle \psi_G|\vec{\mu}^{e}_{mag}|\psi_G\rangle + \vec{\mu}^{n}_{mag}|\chi_{Ge}\rangle\end{aligned} \quad (6)$$

where $|\psi_G\rangle$ is the electronic ground-state wave function, which has the electronic coordinates as variable and depends parametrically on the nuclear coordinates, and $|\chi_{Gk}\rangle$ is the nuclear wave function of the kth vibrational level in electronic state G.

Both nuclear and electronic components of the electric transition-dipole moment [Eq. (5)] can be calculated using Born-Oppenheimer (BO) wave functions. The expressions for the individual terms in Equation (5) are well understood and a complete derivation can be found elsewhere.[1] However, the electronic contribution to the magnetic transition-dipole moment [Eq. (6)] is identically zero within the BO approximation.[9] This follows from the hermitian and imaginary nature of the $\vec{\mu}^{e}_{mag}$ operator together with the non-degeneracy of G.[8] Hence, $\langle \psi_G|\vec{\mu}^{e}_{mag}|\psi_G\rangle = 0$, leading to a scenario where only the nuclei would contribute to the magnetic transition-dipole moment. Hence, to evaluate the contribution of the electrons to the magnetic transition-dipole moment, an expansion of the theory beyond the BO approximation is required.

2.3.1. A Vibronic Coupling Mechanism

To obtain more accurate wave functions, we employ first-order perturbation theory using the terms of the nuclear kinetic energy operator that are neglected in the BO approximation as the perturbation Hamiltonian and the BO wave functions as zero-order expansion functions. With these corrected wave functions, a nonzero electronic contribution to the magnetic transition-dipole moment associated with the transition $\Psi_{Gg} \rightarrow \Psi_{Ge}$ is obtained, which is given by Equation (7):[10]

$$\begin{aligned}&\langle \Psi^{cor}_{Gg}|\vec{\mu}^{el}_{mag}|\Psi^{cor}_{Ge}\rangle = \\ &\langle \chi_{Gg}|\sum_{K\neq G}\frac{\langle \psi_G|\vec{\mu}^{el}_{mag}|\psi_K\rangle}{W^0_K - W^0_G}(\langle \psi_K|T^{(1)}_n|\psi_G\rangle - \langle \psi_G|T^{(1)}_n|\psi_K\rangle)|\chi_{Ge}\rangle\end{aligned} \quad (7)$$

where W^0_K is the electronic energy for the Kth state and $T^{(1)}_n$ is a nuclear kinetic energy operator. The vibronically induced mixing of BO wave functions expressed in Equation (7) is the essence of the mechanism through which VCD signals gain intensity. It shows that electronic magnetic transition-dipole moment can be "borrowed" from electronic transitions due to mixing of BO states. In terms of the classical picture of Section 2.1, a larger current is generated in the coil, since the vibrating nuclei induce a change in the electronic wave function. Equation (7) also shows that this electronic contribution depends strongly on the excitation energies of states from which magnetic transition dipole moment is borrowed. In fact, the theory as expressed in Equation (7) leads one to expect that in systems with low-lying electronically excited states an enhancement of VCD signal intensities might occur compared with analogous systems in which these low-lying electronic states are absent.

2.4. Quantum-Chemical VCD Calculations

Although formally correct, Equation (7) has considerable drawbacks for practical purposes, as it can only be evaluated if the sum over the electronically excited states is truncated at some

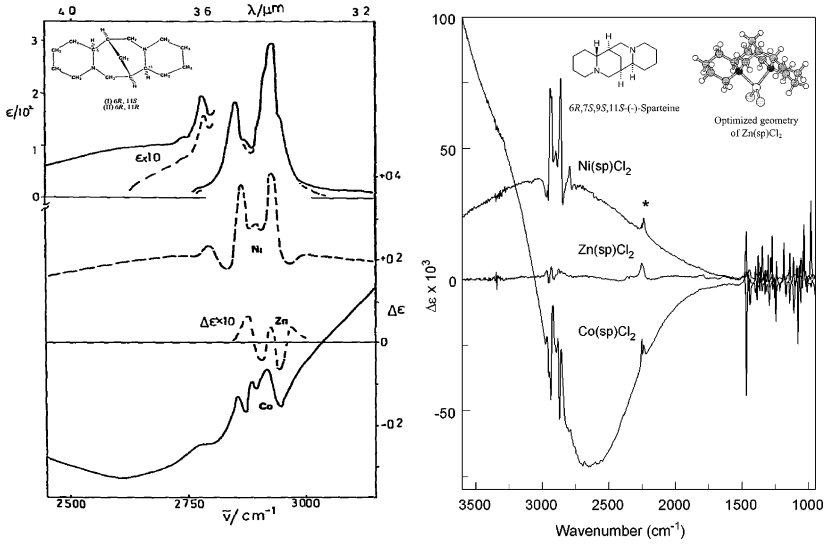

Figure 2. Left: The IR absorption (upper curves) and circular dichroism spectra (lower curves) of [D_3]chloroform solutions of [Co(l-sp)Cl_2] (full curves), [Ni(l-sp)Cl_2] (dashed curves), and [Zn(l-sp)Cl_2] (dash-dot curves). The absorption spectrum of [Zn(l-sp)Cl_2] is distinct from those of the Co^{II} and Ni^{II} analogues, which are identical on the scale presented, only at the band edges outside the C–H stretching vibration region. Reproduced by permission from Ref. [13]. Copyright 1980 of Elsevier. Right: Observed VCD spectra of Zn(sp)Cl_2, Co(sp)Cl_2, and Ni(sp)Cl_2 in the 3600–950 cm^{-1} region, 0.1 mm path length cell, 5 h collection for the sample and solvent, with the instrument optimized at 3000 cm^{-1}. The asterisk indicates an artifact arising from atmospheric CO_2. Reproduced by permission from Ref. [17]. Copyright 2001 of the American Chemical Society.

point. This problem was tackled successfully by P. J. Stephens[11] who has shown that the sum over states expression can be rewritten to an expression involving the derivative of the ground state wave function with respect to nuclear displacement and the derivative of the ground state wave function with respect to a magnetic field perturbation. This magnetic field perturbation (MFP) theory is the theory that has been implemented in Gaussian and ADF quantum chemical packages for the calculation of VCD intensities.

In deriving Equation (7) and the MFP theory it is assumed that electronic wave functions vary slowly with nuclear displacements from the equilibrium geometry. This is reasonable for closed-shell organic molecules with non-degenerate ground states that are well-separated from the lower electronically excited states. However, if we consider metal-organic systems with open-shell configurations that can give rise to many low-lying electronically excited states, these approximations may very well break down. Also, in both cases it is assumed that vibronic energies (that is, electronic plus vibrational energies) can be replaced by electronic excitation energies. For systems in which the lower electronically excited states have energies comparable to vibrational energies, this is clearly not the case. Equation (7) thus provides only a qualitative assessment of the role of the various electronic excited states, but a correct description would require an extension of the theory including correction terms that account for such level of vibronic detail, as has been derived by Nafie.[12] An implementation of these equations in quantum-chemical programs is presently in progress.

3. First Observations of Enhanced VCD

In 1980, Barnett et al.[13] reported the VCD spectra of complexes consisting of a transition-metal ion and the chiral chelating ligand (−)-sparteine in the C–H stretching range (Figure 2, left). Comparison of the VCD spectra for the Zn^{II}, Co^{II} and Ni^{II} complexes reveals small VCD peak intensities for the zinc complex, but extraordinarily large signals for the cobalt and nickel complexes. The explanation of large VCD intensities was tentatively formulated in terms of a Fano-type coupling mechanism,[14] based on the overlap of vibrational transitions with the d-d electronic transitions of Co^{II} and Ni^{II}. In 1992, a similar VCD enhancement was observed by Bormett et al.[15] for the antisymmetric stretch of azide-ligated site-directed mutant hemoglobins and myoglobins (see Figure 3). In Figure 3 we show IR and VCD spectra in the N_3 stretching region for a series of heme protein complexes. The bisignate IR absorption is due to both the ionically bound high-spin azide and the covalently bound low-spin azide with differences in intensities reflecting the differences in the spin state equilibrium between the various proteins. The VCD intensity of the N_3 stretching mode varies depending on heme and bound azide ligand interactions with the distal heme pocket. The large VCD signals observed for some complexes suggests that the source of the enhanced VCD could be due to a vibrationally induced current by the delocalized electrons in the heme plane, but in the absence of further experimental support this explanation remains tentative. This study was followed by a report that demonstrated similar effects in non-heme metalloenzymes.[16]

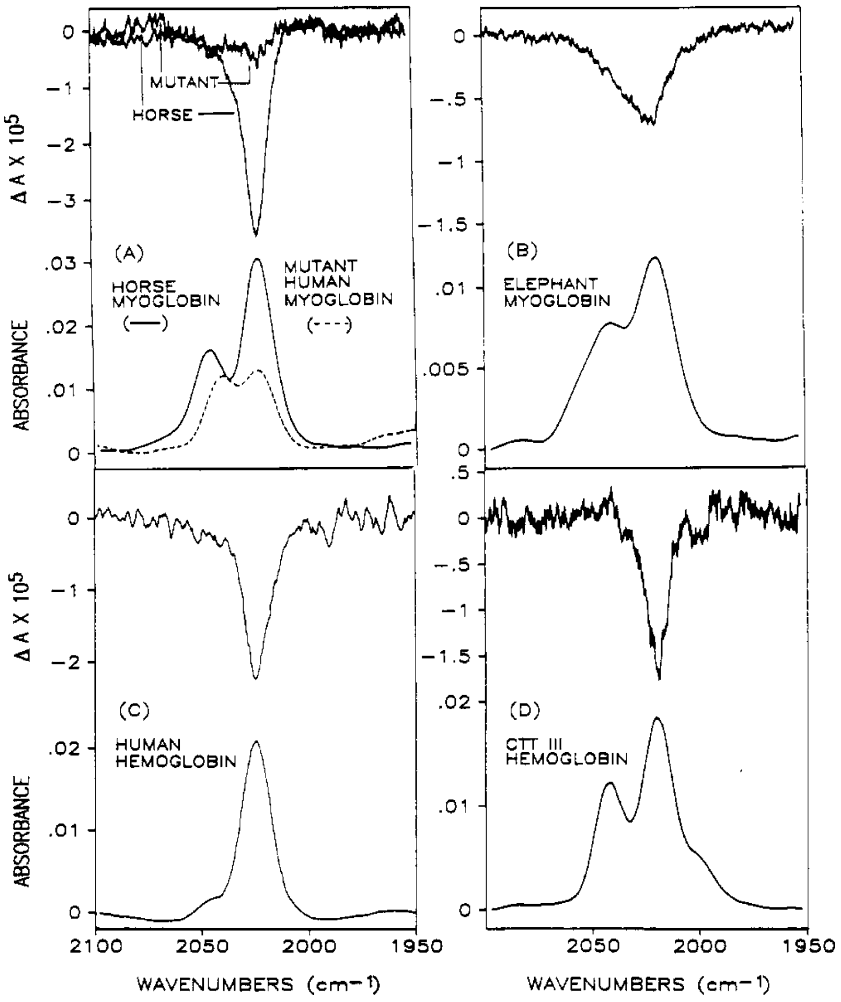

Figure 3. IR absorption (8 cm^{-1} resolution) and VCD (6 cm^{-1} resolution) spectra of: A) 11.5 mM horse MbN_3, and 7.1 mM mutant (Asn E11) human MbN_3, with 2.7 mM unbound N_3^-; B) 6.0 mM elephant MbN_3; C) 8.0 mM human HbN_3; D) 6.0 mM CTT III HbN_3, pH 7 with 0.01 M phosphate buffer adjusted to an ionic strength of 0.7 with KCl. All spectra were measured in a 26-μm CaF_2 cell, and contributions from uncomplexed azide were numerically removed. Reproduced by permission from Ref. [15]. Copyright 1992 of the American Chemical Society.

In 2001, Nafie and co-workers[17] accurately reproduced the results of Barnett et al. in the C–H stretching region (Figure 2, right) of the sparteine complexes but at the same time extended their investigation studies to the 6 μm region, where they also observed large signal enhancements for fingerprint vibrational transitions. Only then a full explanation for the VCD enhancement in terms of low-lying electronically excited states was provided and the pertaining theoretical expressions for the VCD intensities were developed. Since then, Johannessen and Thulstrup,[18] Sato et al.[19] and Merten et al.[20] have reported similar VCD amplification effects in chelating chiral ligands coordinated to transition metals, and rationalized them in part by invoking vibronic coupling with low-lying electronically excited states. As an example, Figure 4 shows the IR and VCD spectra of the spin-triplet bis(biuretate) cobalt(III) complex reported by Johannessen and Thulstrup.[18] Comparison of the IR and VCD spectra in the 6 μm (Figure 4, upper panel) and 3 μm (Figure 4, lower panel) regions for both the free ligand and the cobalt complex reveals a clear enhancement of the intensities in the VCD spectrum of the complex. In the 6 μm region an overall amplification is observed, while in the 3 μm region a broad electronic absorption band is observed, which is assigned to an electric dipole-forbidden, but magnetic dipole-allowed, low-lying d-d transition. Here, the cobalt(III) complex exhibits a square planar coordination geometry with an open-shell electronic configuration and low-lying electronically excited states. This result further suggested that the enhancement of VCD signals caused by coupling of the vibrational transitions to electronic transitions to low-lying electronically excited states.

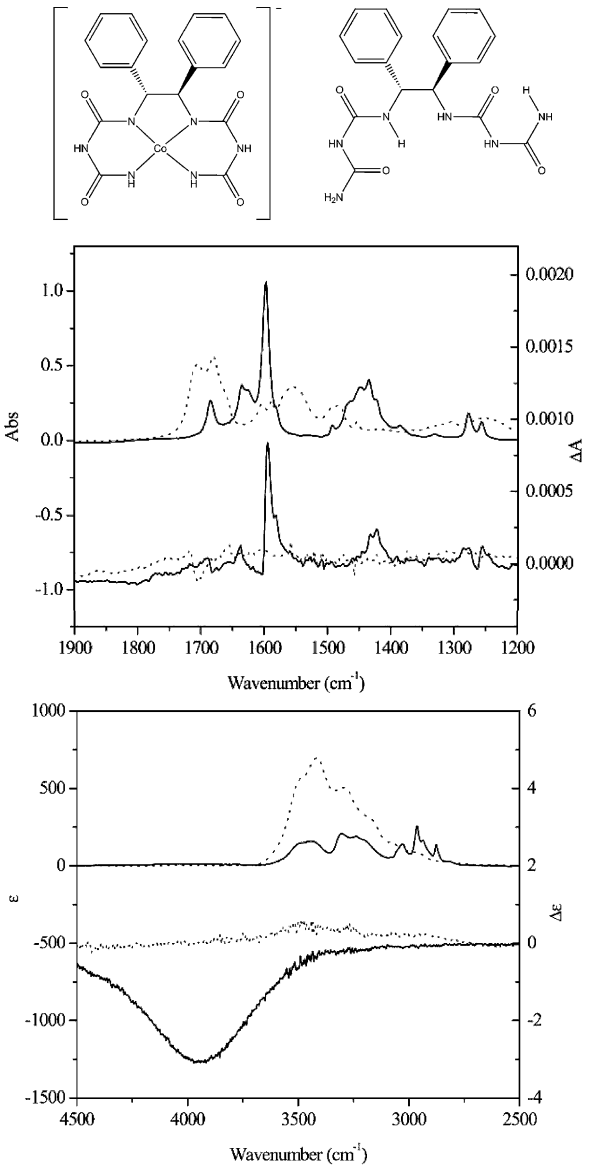

Figure 4. Upper scheme, left: Molecular structure of the (6*S*,7*S*)-1,3,5,8,10,12-hexaaza- 2,4,9,11-tetraoxo-6,7-diphenyl-dodecanato(4-)cobaltate(III) anion. Right: The free ligand, stabilized by intramolecular hydrogen bonding. IR absorption and VCD spectra of the coordination compound (——) and free ligand (-----) in the 6 μm region (middle panel), and in the 3 μm region (lower panel). Adapted with permission from Ref. [18]. Copyright 2007 of the Royal Society of Chemistry.

4. On the Manipulation of the Electronic Manifold and the Amplification of VCD

Previously reported cases of enhanced VCD intensity were observed for molecular systems with rather exotic molecules and rigid molecular coordination spheres of chiral chelating ligands bound to open-shell transition-metal ions. In the following sections, we will show that the amplification of VCD is not limited to such systems, and more importantly, that one can induce amplification of VCD intensities by manipulating the electronic structure of the molecules in a controlled manner, such that low-lying electronic states are "created" that are prone to lead to strong vibronic coupling and thereby to an amplified VCD response.

4.1. Electrochemically Generated Radical Anions

Aromatic compounds undergo one-electron reduction if an electron is transferred to an unoccupied π^* orbital. The resulting radical anions have an open-shell electronic configuration with lower-lying electronically excited states compared with that of their neutral counterparts. Based on this idea, we have developed a novel approach to amplify VCD signals by modulating the energies of the excited-state manifold in a controlled manner using spectroelectrochemistry.[21] For this purpose, an optically transparent thin-layer electrochemical cell (OTTLE) was designed and constructed to perform spectroelectrochemical-VCD measurements using a commercially available VCD spectrometer. The technical details of the experimental setup can be found elsewhere.[22]

To investigate the effect of electrochemical reduction on the VCD response, compounds (*S*)- and (*R*)-methyl 2-(1,3-dioxo-1*H*-benzo[de]isoquinolin-2(3*H*)-yl)propanoate ((*S*)-**1** and (*R*)-**1** respectively, see Figure 5) were investigated in both the neutral and radical anion forms, using UV/Vis, IR and VCD spectroscopy. As expected, the UV/Vis absorption spectrum (Figure 6) of the radical anion shows absorption bands at much longer wavelengths than the corresponding spectrum of the neutral

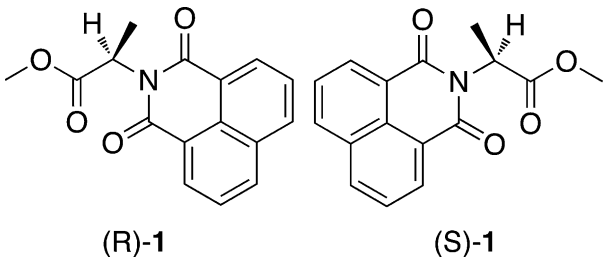

Figure 5. Chemical structure of compounds (*R*)-**1** and (*S*)-**1**. Reproduced by permission from Ref. [23]. Copyright 2012 of the Royal Society of Chemistry.

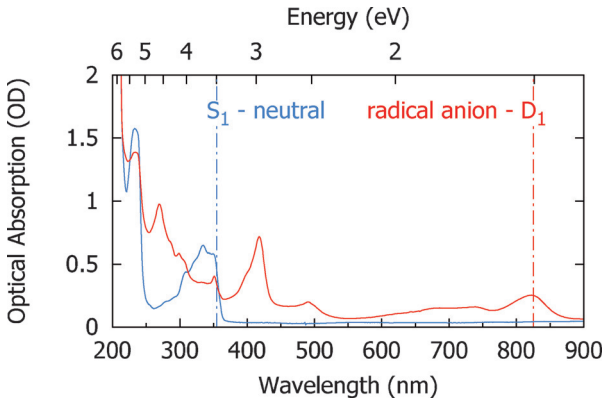

Figure 6. Optical absorption spectrum of (*S*)-**1** in the neutral (blue) and radical anion (red) forms. Reproduced by permission from Ref. [23]. Copyright 2012 of the Royal Society of Chemistry.

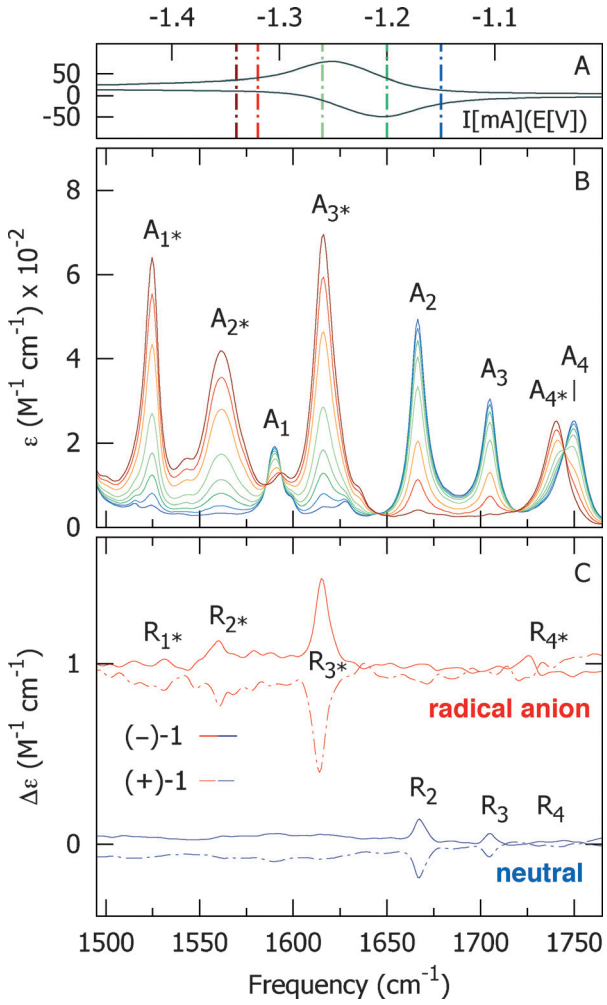

Figure 7. A) Thin-layer cyclic voltammogram of (−)-**1** obtained using the IR OTTLE cell.[21] B) Potential-dependent steady-state IR spectra of 35 mM (−)-**1** (optical path = 200 μm). The blue and red curves represent the spectra of the initial (neutral) and final state (radical anion), respectively. C) VCD spectra of 7 mM (−)-**1** (solid-line) and 7 mM (+)-**1** (dashed-line) (optical path = 1.2 mm) for the neutral (blue) and radical anion (red) species. For clarity, the spectra for the radical anion have been offset vertically. Reproduced by permission from Ref. [23]. Copyright 2012 of the Royal Society of Chemistry.

compound. The observed electronic structure was confirmed by time-dependent density-functional theory calculations.[23]

The IR and VCD spectra of the two forms are displayed in Figure 7. A peak to peak comparison of the VCD peak intensities for neutral and radical-anion forms of **1** shows up to one order of magnitude VCD signal enhancements for the latter form. Interestingly, one has to conclude that these signal enhancements are not the same for all bands. For the C=O stretching modes of **1** a tenfold amplification is found, whereas for the ring and methyl-ester modes the amplification is small or negligible. These differences are directly related to the induced mixing of electronically excited states with the vibrational manifold of the molecules and thus provide valuable information on the finer details of the influence of the lower-lying electronic states. In fact, time-dependent density-functional theory (TD-DFT) calculations predict that it is especially the D_2 state that is expected to be involved in lending the magnetic transition dipole moment to vibrational transitions. Electron difference density plots between D_0 and D_2 show that major changes occur in the electron density on the carbonyl groups and much less on other parts of the molecule. One therefore indeed expects amplification for the C=O stretching modes and much less for other modes.

The same calculations allow us to make a quantitative prediction of the amplification factor using the electronic energy gap between the ground and lower electronically excited states for the neutral and radical-anion species and the magnitude of the magnetic transition-dipole moment for transitions between the ground and electronically excited states [see Eq. (7)]. Using these quantities, the expected amplification of the VCD signals is predicted to be approximately one order of magnitude, which nicely reproduces the observed VCD enhancements and provides further confirmation that the VCD enhancement is due to vibronically induced mixing of low-lying electronically excited states with the ground state.

4.2. Biomolecules Surrounding Paramagnetic Metal Ions

In the previous section, electrochemistry has been used to change the electronic manifold of the compound of interest and optimize it for enhancing VCD signal intensities. Bearing in mind that key to this enhancement is the presence of low-lying electronically excited states, one could very well imagine

that such states can also be introduced by coupling the molecule of interest—which by itself might not have such states—to an auxilliary that does possess low-lying electronically excited states. We have demonstrated the effectiveness of such an approach in experiments on amino acids and peptides under biological conditions[24] for which normally only weak VCD signals are observed. To provide suitable conditions for VCD enhancement, the electronic manifold was altered by actively binding amino acids and peptides to a paramagnetic metal ion (Co^{II}). Interestingly, the thereby created situation closely resembles that of a binding pocket of a protein in which ligands are coordinated around the metal. These studies showed gigantic signal enhancements (up to two orders of magnitude) in the VCD spectra of various amino acids such as alanine, proline and valine (Figure 8), and an approximately tenfold amplification for di- and tripeptides (Figure 9). As an example, we show in Figure 8 the infrared absorption (A, upper panel) and VCD (A, lower panel) spectra of a $[Co^{II}(Pro)_2(D_2O)_2]$ (Pro = proline) complex (colored lines) and of the uncomplexed proline molecule (black lines). The IR spectra confirm complexation of proline with Co^{II} since a splitting is observed for the carboxylate stretching mode as a consequence of exciton coupling between pairs of prolines in the complex. Of special interest in Figure 8 A is the inset which shows sharp vibrational bands, but also a much broader band spanning several hundreds of wavenumbers. This band can be assigned to magnetic-dipole allowed d-d transitions of Co^{II} in agreement with previous experiments.[17,18] Its observation strongly suggests that vibronic coupling plays a dominant role in VCD amplification, but by itself does not yet provide conclusive evidence for it. Definite proof is provided by the VCD spectra of proline–cobalt complexes with the metal center in its diamagnetic Co^{III} state. In this state, the electronically excited states of Co are at much higher excitation energies, and one would therefore expect significantly smaller VCD signals. This expectation is nicely borne out in experiments (Figure 8 B) that show a complete absence of VCD amplification under these conditions.

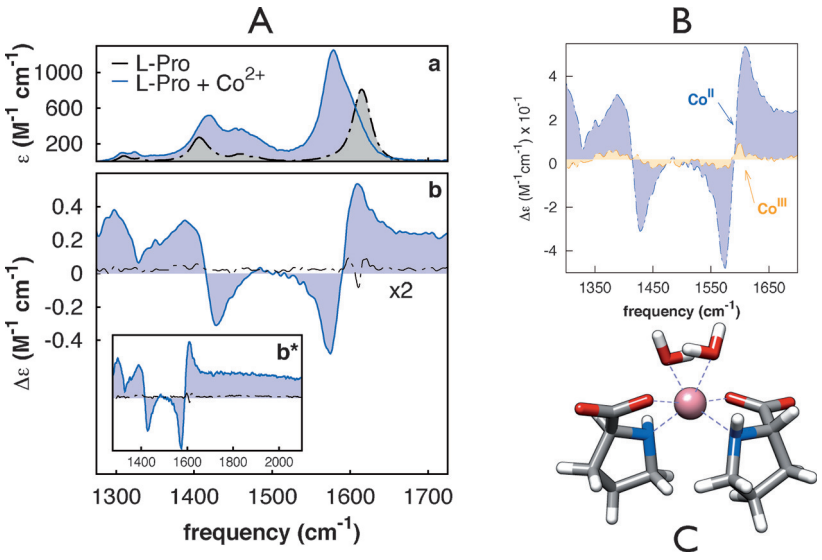

Figure 8. A) IR absorption and VCD spectra of L-proline (a,b) in D_2O (black dashed lines) and of the $[Co^{II}(Pro)_2(D_2O)_2]$ complex (solid filled lines). The sample was prepared in D_2O ($c \approx 25$ mM). The VCD spectra of the amino acid and of the complex were averaged with 4320 scans (1 hour) at a resolution of 4 cm^{-1}. The VCD spectra of the amino acid (dashed lines in b) have been scaled for better comparison with the enhanced VCD spectrum of the complex. The inset b* displays an extension up to 2100 cm^{-1} of the spectrum depicted in b. B) Experimental VCD spectra of $[Co^{II}(Pro)_2(D_2O)_2]$ (in blue) and $[Co^{III}(Pro)_2(D_2O)_2]$ (in orange) complexes. C) Molecular structure of $[Co^{II}(Pro)_2(D_2O)_2]$. Reproduced by permission from Ref. [24]. Copyright 2014 of the American Chemical Society.

4.2.1. Mode-Selective VCD Enhancement

Many biomolecules, such as metalloproteins, contain transition-metal ions as part of their active site. The spatial structure of these metal binding pockets is often directly related to the biological functionality of the system; having access to this structure is thus of primary importance to understand this functionality. Interestingly, it turns out that the intensity and the shape of the amplified VCD signals in combination with the spectral information contained in the IR spectra is a powerful means to retrieve the coordination geometries of polypeptides with metal ions.[24] To illustrate this, we show in Figure 9 IR absorption and VCD spectra of bare di- and tripeptides (dashed-black) and of the same peptides bound to the metal ion auxiliary (full-colored). Comparison of the signal intensities of the bands in the VCD spectra show: 1) that VCD bands are strongly amplified for the Co^{II}-coordinated peptides and 2) that this amplification is strongly mode-dependent. We observe, for example, for the dipeptide that the carboxylate mode at 1580 cm^{-1} is not amplified at all in the VCD spectrum, while the amide I mode—which shifts from 1650 to 1610 cm^{-1} upon complexation—is amplified by more than an order of magnitude. These observations demonstrate that binding of the dipeptide does not involve the carboxylate group and occurs in such a way that the carbonyl stretch directly affects the electronic manifold of the Co ion. The only binding configuration that can be reconciled with these requirements is the one depicted next to Figures 9 a and b. The IR and VCD spectra of tripeptides (see Figure 9) show that the spatial resolving power of this approach goes even further. From the IR spectra (see Figure 9 c) it can be concluded that the two amide moieties of the tripeptide do not interact equally with the Co^{II} center: upon coordination, the amide I band 1 is shifted by 40 cm^{-1} to the red (band 1′), while the amide I band 2′ is only shifted by 3 cm^{-1} from its non-complexed counterpart band 2. Apart from different frequency shifts, the two bands also exhibit a very different amplification of their intensity in the VCD spectrum. This observation indicates that the electronic manifold of the Co^{II} ion is much more susceptible to the carbonyl stretch

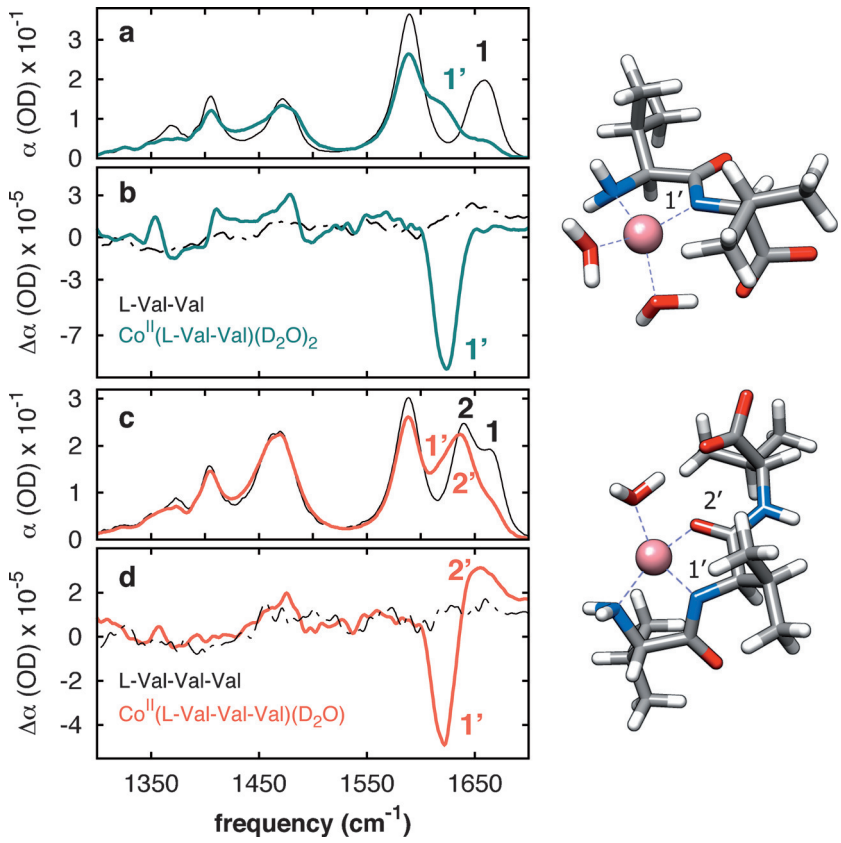

Figure 9. IR absorption (a) and VCD (b) spectra of L-Val-Val (black lines) and [Co^{II}(L-Val-Val)(D_2O)$_2$] (green lines) and IR absorption (c) and VCD (d) spectra of L-Val-Val-Val (black lines) and [Co^{II}(L-Val-Val-Val)(D_2O)] (red lines). The numbered IR bands in panels (a) and (c) correspond to the VCD bands in panels (b) and (d), respectively. The numbered moieties in the molecular structures of the Co^{II} bound valine dipeptide (high-spin) and Co^{II} bound valine tripeptide (high-spin) correspond to the numbered peaks in the VCD spectra. Reproduced by permission from Ref. [24]. Copyright 2014 of the American Chemical Society.

involved in modes 1 and 1′ than the one associated with modes 2 and 2′. This, in turn, leads to the conclusion that the tripeptide is bound to the Co^{II} ion in the configuration shown in Figure 9.

4.3. Probing Local Structure: Cutting through a Congested VCD Spectrum

A detailed understanding of the relation between molecular structure and functionality requires the ability to zoom in on specific parts of a molecular system. The selective enhancement of VCD signals in the vicinity of metal ions discussed in the previous section seems well suited for this purpose, but for larger molecular systems, its usefulness rapidly deteriorates because all parts of the molecule contribute to the VCD spectrum. As a result, very congested spectra are obtained from which it is hard—if not impossible—to extract information on amplified modes. To address this problem, we have devised a novel methodology based on the concept of a switchable local VCD amplifier.[25] The amplifier is in this case a molecular entity that can be covalently coupled to a user-defined part of a molecule and that can be switched on and off electrochemically using the VCD-OTTLE cell. The first experimental demonstration of this methodology has been performed using ferrocene (Fc) as the VCD amplifier. In the neutral form (Fe^{II}), ferrocene has a closed-shell electronic configuration with electronically excited states well separated from the electronic ground state. The one-electron-oxidized ferrocenium cation, in contrast, has an open-shell configuration (Fe^{III}) with low-lying electronically excited states. Adjusting the electrochemical potential thus allows alternation between so-called ON and OFF configurations: the ON configuration generates an electronic manifold with low-energy electronically excited states that "activate" VCD signal amplification, whereas the OFF configuration turns off the amplification by returning the electronic manifold to its original configuration without low-lying electronically excited states. Subtraction ($\Delta\alpha_{ON} - \Delta\alpha_{OFF}$) of VCD spectra now directly isolates the normal modes which undergo VCD amplification, and eliminates signals associated with regions outside the spatial amplification range that would otherwise overwhelm the VCD spectrum. The validity of this concept has been demonstrated on di- and tripeptides. Figure 10 (left) and Figure 11 (left) show infrared absorption and VCD spectra of the di- and tripeptides, respectively, in the OFF (solid lines) and ON (dashed lines) configurations. An overall amplification in the ON configuration is perceptible through comparison of its VCD intensities with those recorded for the OFF configuration. Moreover, modes that fall outside the spatial range over which the amplifier is active are eliminated in the difference spectrum.

4.3.1. *Distance Dependence of the Amplification Effect*

The studies described above clearly indicate that the amplification of VCD signals is strongly dependent on the distance from the amplifying entity. To quantify this distance dependence—and thereby determine an effective amplification range—we have measured amplification factors of localised modes that are increasingly further away from the VCD amplifier. The AA dipeptide shown in Figure 10 features two amide I vibrational modes (Ala_1 and Ala_2) and one methyl ester C=O stretching mode (Ala_3) whereas the APA tripeptide shown in Figure 11 exhibits three amide I vibrational modes (Ala_1, Pro_2 and Ala_3) and one methyl ester C=O stretching mode (Ala_4). The subscripts in these designations correspond to the labeled groups and the

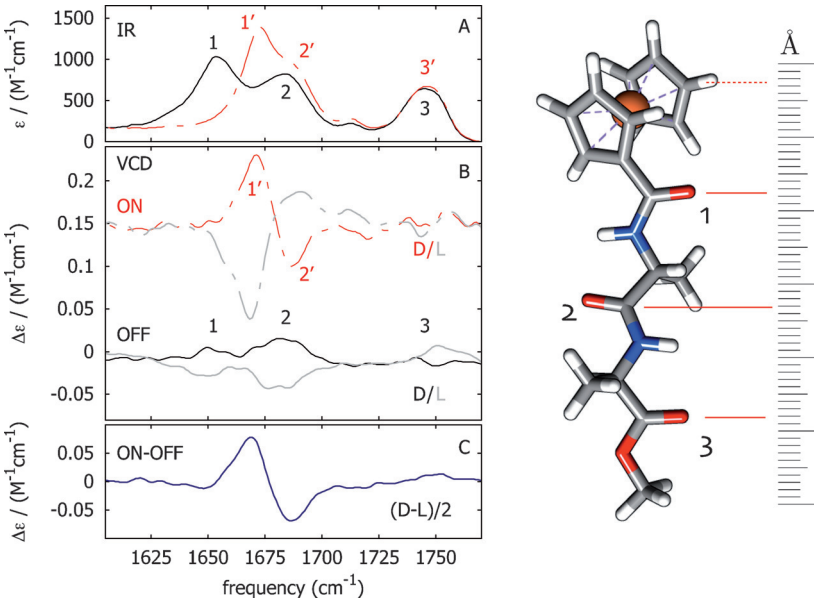

Figure 10. Left: IR (A) and VCD spectra (B) of 10^{-2} M Fc-(L/D)-Ala-Ala-Ester in CD_3CN (10^{-1} M Bu_4NPF_6, 200 μm optical pathlength). The VCD spectra of the ON configuration have been offset for clarity. Panel C displays the difference spectrum of the VCD spectra in the ON and OFF configurations. Right: Molecular structure of Fc-(L)-Ala-Ala. A schematic ruler is plotted next to the peptide backbone to highlight the distance between the ferrocene moiety, and the amide and ester groups. Reproduced by permission from Ref. [25]. Copyright 2014 of Wiley-VCH.

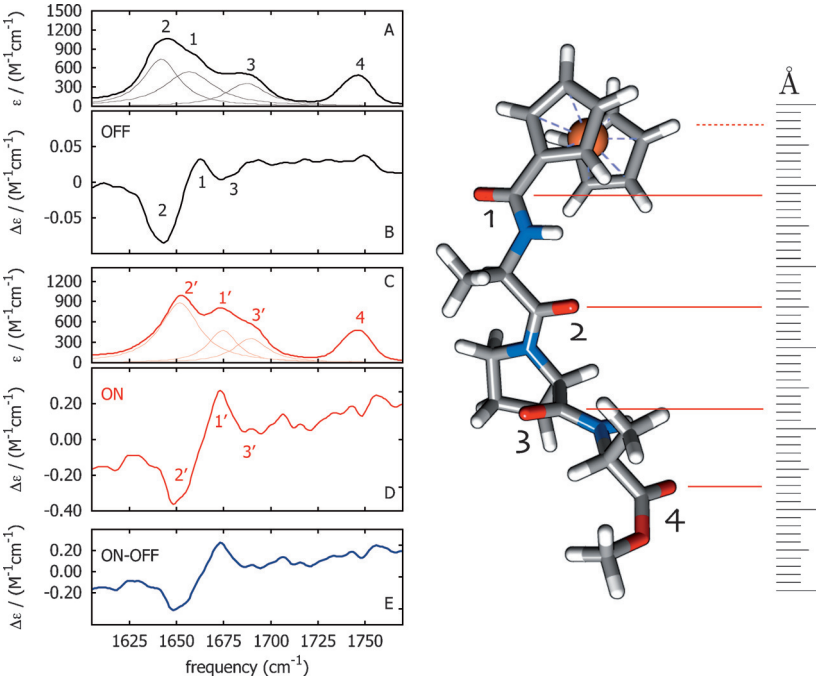

Figure 11. Left: IR (A,C) and VCD spectra (B,D) of 10^{-2} M Fc-(L)-Ala-Pro-Ala in CD_3CN (10^{-1} M Bu_4NPF_6, 200 μm optical pathlength), for the OFF and ON configurations, respectively. Panel E displays the difference spectrum of the VCD spectra in the ON and OFF configurations. Right: Molecular structure of Fc-(L)-Ala-Pro-Ala. A schematic ruler is plotted next to the peptide backbone to highlight the distance between the ferrocene moiety, and the amide and ester groups. Reproduced by permission from Ref. [25]. Copyright 2014 of Wiley-VCH.

corresponding normal modes in the IR and VCD spectra, and have been chosen in order of the increasing distance from the amplifier. All modes have well-separated frequencies, which allows for a better comparison of signal intensities and amplification factors. A direct measure of the amplification factor for each vibrational mode can be obtained by determining the anisotropy factor ($g = \Delta\varepsilon/\varepsilon$) for each individual normal mode in the ON and OFF configurations. In Figure 12 the amplification factor, defined as g'/g ($g \rightarrow$OFF, $g' \rightarrow$ON), is plotted as a function of the distance of the normal mode to the amplifier. A fit to the data points by using the function $1 + Ae^{-x/R_0}$, where x is the distance (in number of bonds) between the chemical group and the amplifier, shows that the amplification is reduced by a factor of $1/e$ for normal modes at a characteristic distance, R_0, of 2.0 ± 0.3 bonds from the amplifier. In a simplified picture all parts of the molecule that are located further than two covalent bonds away from the amplifier will thus not undergo any meaningful VCD-intensity amplification. Put in another way, one might say that the switchable VCD amplifier allows us to zoom in on a region in space equivalent to a sphere around the amplifier with a radius of two bond lengths Although this result might vary depending on the type of bond or its spatial orientation, this result clearly demonstrates the potential of amplified VCD as a probe of local structure.

5. Outlook

Vibrational circular dichroism has come of age since its first experimental observation in 1973. In particular, it has become clear that VCD has tremendous potential as a spectroscopic tool in the investigation of molecular stereochemistry in general, and of chirality in biomolecular systems in particular. Nevertheless, it has also become clear that there is still much to gain, primary targets in this respect being the ability to overcome the intrinsic small-signal limitations of VCD and the ability to zoom in on user-defined regions of large molecular systems. This is an am-

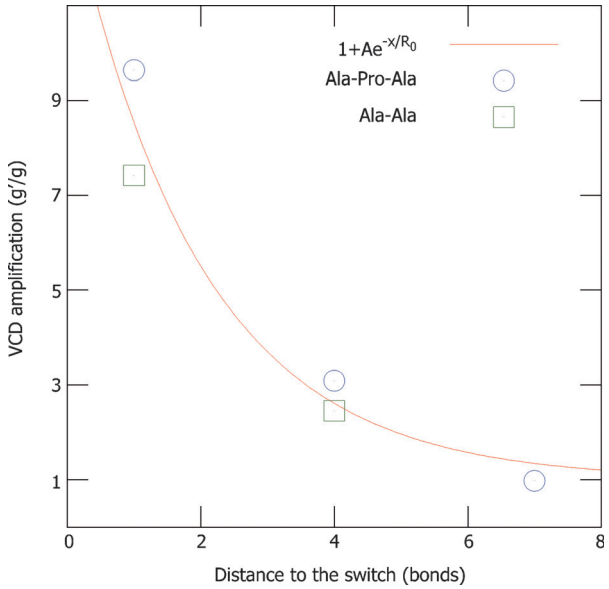

Figure 12. VCD amplification factors (g'/g) as a function of the distance (number of covalent bonds) from the electroactive group to each of the indicated functional groups of Fc-(L)- Ala-Ala and Fc-(L)-Ala-Pro-Ala. Reproduced with permission from Ref. [25]. Copyright 2014 of Wiley-VCH.

bitious goal, but one that nowadays is coming within reach, as demonstrated by the studies on vibronically induced amplification of VCD signals that we have described in this Concept article. These studies have shown that as far as signal intensities are concerned it is possible to manipulate electronic manifolds in such a way that circular dichroism associated with nuclear motion is essentially coupled to electronic circular dichroism, thereby putting VCD and ECD on equal footing. One aspect that we have not been touched upon so far is the comparison between experimentally recorded and theoretically predicted VCD spectra, which traditionally has been the stronghold for extracting the maximum amount of structural information possible from experimental VCD spectra. VCD studies by us and others show that the MFP-based theoretical description derived by Stephens, which is currently implemented in quantum chemical programs, does not suffice. In fact, these studies clearly indicate that the stronger the influence of low-lying electronically excited states, the larger the differences between experimental and theoretical spectra. To correctly describe VCD spectra under low-lying excited-state conditions, a different approach needs to be adopted in which the theory is extended as to include vibronic detail. The appropriate equations have recently been derived.[12] Once these equations are implemented—and this is currently underway—it will be possible to use VCD signal amplification not only in a qualitative way, but also to derive a quantitative structural information, thereby opening a new research territory. The concept of a local VCD amplifier offers a plethora of possibilities to study binding pockets and active sites of proteins and enzymes. Our initial studies on model systems indicate that implementation of such an amplifier by coupling it to user-defined location within a molecule should provide unprecedented structure elucidation at the local scale. As a perspective for the future, Figure 13 shows a schematic outlook for the application of locally amplified VCD for the investigation of site-specific chiral molecular targets. The highlighted region of the molecule contains an electroactive group which is embedded within the molecule. Subtracting the VCD spectra in the ON and OFF states of the amplifier then gives rise to signals that are exclusively associated with oscillators in the vicinity of the electroactive group, and effectively enables us to turn VCD into a zero-background technique (subtraction of the ON and OFF VCD spectra leads to null signals for spatial regions not connected to the switch). Local VCD amplification thus paves the way towards a unique manner of spectrally resolving protein local structure in solution.

In many aspects, the concept of a switchable local amplifier resembles that of a molecular beacon: a probe that can be placed in a key location within the molecule, and be externally controlled to illuminate that specific part of the molecule and its surroundings. It should be emphasized that in principle any molecular entity with a suitable electronic configuration can be used as an auxiliary, thereby generating a local environment where the necessary conditions for VCD amplification are at work. Switchable amplifiers thus do not necessarily need to be electroactive entities, but can also be based on other types of switches. Our findings regarding the localized nature of the VCD enhancement greatly extend the possible applications of VCD to locally elucidate the chiral structure of functional biomolecules under biologically relevant conditions which are inaccessible with other techniques under similar conditions.

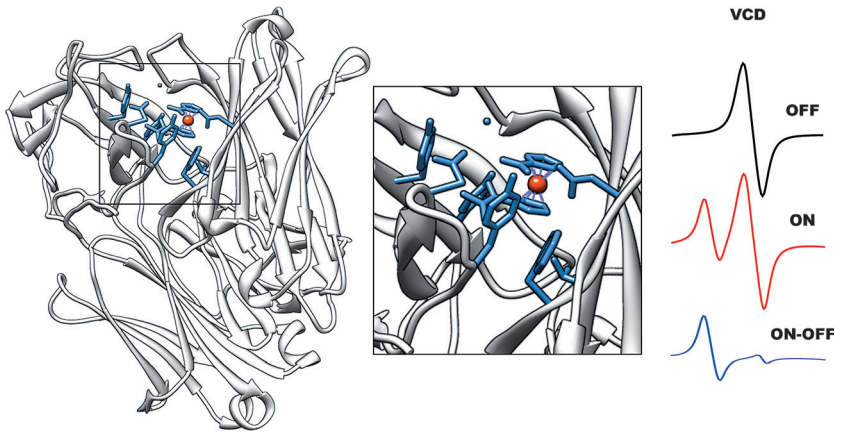

Figure 13. Schematic figure demonstrating amplified VCD as a zero-background technique using ON/OFF subtraction to zoom in into specific regions of large biomolecular systems. This protein, catalytic antibody Fab 1345 (PDB 1A3L), contains a ferrocene moiety in its active site.

Acknowledgements

The authors thank Professors Bas de Bruin and Larry Nafie for their insights and helpful discussions and Bert H. Bakker, Michiel F. Hilbers, Hans J. Sanders, Henk Luyten, and Fred van Anrooij for the synthetic work and technical support. S.R.D. acknowledges financial support from the Portuguese Foundation for Science and Technology (FCT) under the fellowship SFRH/BD/48295/2008. S.W. acknowledges the European Research Council (ERC) for funding through Grant No. 210999. F.H. thanks the University of Reading for the support of the Reading Spectroelectrochemistry laboratory (Project D14-015).

Keywords: biomolecules · chirality · circular dichroism · local amplification · structure elucidation

[1] L. A. Nafie, *Vibrational Optical Activity: Principles and Applications*, Wiley, Chichester, **2011**.
[2] P. J. Stephens, F. J. Devlin, J. R. Cheeseman, *VCD Spectroscopy for Organic Chemists*, CRC Press, Taylor & Francis Group, Boca Raton, FL, **2012**.
[3] L. A. Nafie, T. A. Keiderling, P. J. Stephens, *J. Am. Chem. Soc.* **1976**, *98*, 2715 – 2723.
[4] M. J. Frisch, G. W. Trucks, H. B. Schlegel, G. E. Scuseria, M. A. Robb, J. R. Cheeseman, G. Scalmani, V. Barone, B. Mennucci, G. A. Petersson, H. Nakatsuji, M. Caricato, X. Li, H. P. Hratchian, A. F. Izmaylov, J. Bloino, G. Zheng, J. L. Sonnenberg, M. Hada, M. Ehara, K. Toyota, R. Fukuda, J. Hasegawa, M. Ishida, T. Nakajima, Y. Honda, O. Kitao, H. Nakai, T. Vreven, J. A. Montgomery, Jr., J. E. Peralta, F. Ogliaro, M. Bearpark, J. J. Heyd, E. Brothers, K. N. Kudin, V. N. Staroverov, R. Kobayashi, J. Normand, K. Raghavachari, A. Rendell, J. C. Burant, S. S. Iyengar, J. Tomasi, M. Cossi, N. Rega, J. M. Millam, M. Klene, J. E. Knox, J. B. Cross, V. Bakken, C. Adamo, J. Jaramillo, R. Gomperts, R. E. Stratmann, O. Yazyev, A. J. Austin, R. Cammi, C. Pomelli, J. W. Ochterski, R. L. Martin, K. Morokuma, V. G. Zakrzewski, G. A. Voth, P. Salvador, J. J. Dannenberg, S. Dapprich, A. D. Daniels, Ö. Farkas, J. B. Foresman, J. V. Ortiz, J. Cioslowski, and D. J. Fox, Gaussian 09, Revision C.02, **2009**, Gaussian, Inc., Wallingford, CT.
[5] A. Theoretical Chemistry, Vrije Universiteit, Amsterdam Density Functional program, URL: http://www.scm.com.
[6] R. P. Feynman, R. B. Leighton, M. Sands, The Feynman Lectures on Physics, AddisonWesley, Reading, **1963**.
[7] I. Tinoco, M. P. Freeman, *J. Chem. Phys.* **1957**, *61*, 1196 – 1200.
[8] P. Atkins, R. Friedman, *Molecular Quantum Mechanics*, Oxford University Press, Oxford, **2005**.
[9] T. R. Faulkner, C. Marcott, A. Moscowitz, J. Overend, *J. Am. Chem. Soc.* **1977**, *99*, 8160 – 8168.
[10] L. A. Nafie, T. B. Freedman, *J. Chem. Phys.* **1983**, *78*, 7108.
[11] P. J. Stephens, *J. Phys. Chem.* **1985**, *89*, 748 – 752.
[12] L. A. Nafie, *J. Phys. Chem. A* **2004**, *108*, 7222 – 7231.
[13] C. Barnett, A. Drake, R. Kuroda, S. Mason, S. Savage, *Chem. Phys. Lett.* **1980**, *70*, 8 – 10.
[14] U. Fano, *Phys. Rev.* **1961**, *124*, 1866 – 1878.
[15] R. W. Bormett, S. A. Asher, P. J. Larkin, W. G. Gustafson, N. Ragunathan, T. B. Freedman, L. A. Nafie, S. Balasubramanian, S. G. Boxer, N. T. YU, K. Gersonde, R. W. Noble, B. A. Springer, S. G. Sligar, *J. Am. Chem. Soc.* **1992**, *114*, 6864 – 6867.
[16] R. W. Bormett, G. D. Smith, S. A. Asher, D. Barrick, D. M. Kurtz, *Faraday Discuss.* **1994**, *99*, 327.
[17] Y. He, X. Cao, L. A. Nafie, T. B. Freedman, *J. Am. Chem. Soc.* **2001**, *123*, 11320 – 11321.
[18] C. Johannessen, P. W. Thulstrup, *Dalton Trans.* **2007**, *10*, 1028 – 1033.
[19] H. Sato, T. Taniguchi, A. Nakahashi, K. Monde, A. Yamagishi, *Inorg. Chem.* **2007**, *46*, 6755 – 6766.
[20] C. Merten, K. Hiller, Y. Xu, *Phys. Chem. Chem. Phys.* **2012**, *14*, 12884 – 12891.
[21] M. Krejčik, M. Daněk, F. Hartl, *J. Electroanal. Chem.* **1991**, *317*, 179 – 187.
[22] S. R. Domingos, H. Luyten, F. van Anrooij, H. J. Sanders, B. H. Bakker, W. J. Buma, F. Hartl, S. Woutersen, *Rev. Sci. Instrum.* **2013**, *84*, 033103.
[23] S. R. Domingos, M. R. Panman, B. H. Bakker, F. Hartl, W. J. Buma, S. Woutersen, *Chem. Commun.* **2012**, *48*, 353 – 355.
[24] S. R. Domingos, A. Huerta-Viga, L. Baij, S. Amirjalayer, D. A. E. Dunnebier, A. J. C. Walters, M. Finger, L. A. Nafie, B. de Bruin, W. J. Buma, S. Woutersen, *J. Am. Chem. Soc.* **2014**, *136*, 3530 – 3535.
[25] S. R. Domingos, H. J. Sanders, F. Hartl, W. J. Buma, S. Woutersen, *Angew. Chem. Int. Ed.* **2014**, *53*, 14042 – 14045; *Angew. Chem.* **2014**, *126*, 14266 – 14269.

Manuscript received: July 12, 2015
Final Article published: September 9, 2015